Dislocation multiplication in silicon at the onset of plasticity observed by *in situ* synchrotron x-ray topography

2000 J. Phys.: Condens. Matter 12 10045

(http://iopscience.iop.org/0953-8984/12/49/304)

J. Phys.: Condens. Matter **12** (2000) 10045–10058. Printed in the UK PII: S0953-8984(00)17587-3

Dislocation multiplication in silicon at the onset of plasticity observed by *in situ* synchrotron x-ray topography

Alain Jacques†§, Frédéric Vallino†§, Francisco Serbena‡§ and Amand George†§

† Laboratoire de Physique des Matériaux, UMR CNRS No 7556, Ecole des Mines de Nancy, Nancy, France

‡ Universidade Estadual de Ponta Grossa, Department de Fisica, Ponta Grossa, Brazil

§ European Synchrotron Radiation Facility, BP 220, F-38043 Grenoble, France

Received 13 September 2000

Abstract. *In situ* observations by synchrotron x-ray topography were performed on initially dislocation-free silicon single crystals deformed in creep conditions at temperatures between 975 K and 1075 K, and tensile stresses equal to 22 MPa or 44 MPa, in order to study the multiplication of dislocations during the very first stages of plastic deformation.

It could be seen that the first dislocations, created at Vickers micro-indents or at residual surface damage, did not develop in a strictly planar way: prismatic half loops, gliding simultaneously on two {111} planes, were commonly observed. Cross-slip events appeared to be quite frequent, in the bulk as well as at free surfaces. Groups of similar dislocations soon exhibited irregular shapes with cusps and trailing dipoles, which was taken as an indication that they developed jogs during their motion. Several configurations of dislocation sources formed by the mobile dislocations were observed and are described in detail. The formation of new sources usually involved cross-slip. The role of jogs formed by forest-cutting seems important. The efficiency of sources was strongly limited by the lack of stability of the cross-slipped segments, which acted as poles for the Frank–Read mechanism.

1. Introduction

Dislocation multiplication in deforming crystals proceeds via Frank–Read sources, consisting of mobile dislocation segments bowing out between fixed poles, under the action of shear stresses, so as to form spirals or concentric closed loops of fresh dislocations. Fixed poles, around which mobile segments turn, are assumed to be dislocation nodes of the three-dimensional Frank network, which is present in well annealed metals. In later stages of plastic deformation new sources continuously form due to intersections of primary dislocations with trees having other Burgers vectors.

The first convincing experimental proof of such a Frank–Read source was probably obtained by Dash in silicon [1], in crystals twisted at high temperatures and observed by infrared light after copper decoration of dislocations. Yet, dislocation multiplication during the very first stages of deformation is still poorly understood in present day Si crystals, which, in contrast to those of Dash, are initially dislocation free and do not contain any Frank network.

In their model of the yield stage, Alexander and Haasen [2] used an empirical multiplication law of the form

$$\frac{\mathrm{d}\rho}{\mathrm{d}t} = \dot{\rho} = K\rho v\tau_{eff}$$

0953-8984/00/4910045+14$30.00

where ρ is the dislocation density (all dislocations being taken as mobile), v the average dislocation velocity and τ_{eff}, the effective shear stress exerted on dislocations. This relation was derived from etch pit counts in crept germanium crystals [3], but lacks a clear physical basis. More recently, numerical simulations by Moulin *et al* [4] succeeded in reproducing the most salient features of the yield stage of silicon using the simple assumption of a random distribution of fixed sources of various sizes. This simulation, however, does not fit the multiplication law of Alexander and Haasen.

It is clear to us that a fixed distribution of pre-existing sources is not realistic in dislocation-free silicon and that new sources must be created during deformation by the moving dislocations themselves. Then, in order to study dislocation multiplication at the onset of plasticity, the challenge from the experimental point of view is to follow the evolution of low dislocation densities over large crystal areas. A possibility, which may be the only one, is offered by x-ray topography thanks to high intensity synchrotron radiation sources, which allow us to image dislocations in a few seconds. The paper reports on *in situ* observations made at the ESRF during creep of silicon single crystals.

2. Experiment

Tensile specimens, $15 \times 4 \times 0.7$ mm^3 in size for the gauge length, were cut from FZ undoped silicon wafers with a $(\bar{2}21)$ or (110) surface (respectively 'A' and 'B' orientation). They were diamond and chemically polished in order to remove, with great care, any surface defects which could act as dislocation sources. A few Vickers micro-indents were made to locate original sources. A dual slip $[1\bar{1}4]$ tensile axis was chosen, which has the advantage of avoiding a zero resolved shear stress on the cross-slip plane of primary dislocations, as would have been the case with the conventional [123] single slip orientation. The two different orientations provided different view angles on the dislocations, with primary and cross-slip planes alternatively seen 'flat' or nearly end-on.

The experiments were done at the ID19 beam-line of the ESRF. The specimens were observed in transmission using either $g = \bar{2}20$ or $\bar{2}\bar{2}0$ as the diffracting vector for 'A' and 'B' orientations respectively. Because of the very small divergence of the monochromatized beam and of unavoidable strain gradients in the specimen when loaded, a low amplitude scan in angle θ (typically $\sim 0.1^\circ$) had to be applied to the specimen during the exposure in order to record the image of the whole gauge length. The images were recorded simultaneously on x-ray films and with the CCD FRELON camera (1000×1000 pixels, 10 μm resolution) of the ID19 beam-line. Typical times of exposure varied from 30 seconds to one minute, depending on the scan amplitude. Successive snapshots of expanding dislocation loops were taken every few minutes.

The specimens were strained in creep conditions, at temperatures from 975 K to 1075 K, with applied loads of 22 and 44 MPa, i.e. with shear stresses of 10 and 20 MPa on primary slip systems. The experiments were done under a 5×10^4 Pa argon atmosphere, after careful degassing of the straining stage. Specimens were cooled down with the load applied before the dislocation densities became too high. *Post mortem* Burgers vector analysis was performed by classical Lang topography on that final state.

3. Results

3.1. Origin of first dislocations and activated slip systems

During creep tests, dislocations appeared just after loading around indents and at residual surface damage, usually localized on side faces. From indents, dislocation half-loops formed

in three slip planes (111) and (11$\bar{1}$), primary planes and (1$\bar{1}$1). From surface damage, one or two sets of planes were activated at a given area.

The number of loops emitted from a source area was often limited, in which case a dislocation free zone appeared behind the last emitted dislocation when half-loops increased in size with time.

Ten slip systems out of 12 could be identified in most samples. It turned out that all systems with a non-zero Schmid factor were activated. The Schmid factors of activated systems ranged from $s = 0.18$ to $s = 0.46$ (primary systems).

3.2. Non-planar dislocation configurations

As explained in section 1, dislocation multiplication can only take place in non-planar situations: a dislocation segment must be able to bend and turn around poles made of dislocation lines lying out of its slip plane. Therefore any observations of non-planar slip may be of interest for our problem. Three kinds of non-planar development of dislocation loops were identified during our experiments. These configurations have been described in some detail in [5] and are just listed below.

(i) A first typical configuration is that of a prismatic half-loop developed on the two {111} planes containing the Burgers vector right from the beginning of the loop growth i.e. from the indent, as far as the limited spatial resolution of x-ray topography allows us to judge. This was consistently observed for dislocations of the primary Burgers vectors, $\frac{1}{2}[101]$ and $\frac{1}{2}[0\bar{1}1]$, which have $s = 0.46$ in the primary plane, $(\bar{1}\bar{1}1)$ and (111) respectively, and $s = 0.23$ in the common cross-slip plane, $(\bar{1}11)$, and even more frequently for dislocations with $b = \frac{1}{2}[1\bar{1}0]$, which have the same $s = 0.18$ on their two possible slip planes.

(ii) The second kind of non-planar configuration resulted from cross-slip at a later stage of loop growth. Cross-slip was observed quite frequently, starting in the bulk as well as at the free surface. For example, bulk cross-slip was repeatedly observed on secondary dislocations with $b = \frac{1}{2}[011]$, which developed first in $(1\bar{1}1)$ ($s = 0.41$) and then cross-slipped to $(\bar{1}\bar{1}1)$ ($s = 0.27$). The ease of cross-slip in our experiments appeared to be correlated with the ratio of Schmid factors: the highest s cross-slip/s original plane and the highest cross-slip frequency. Cross-slip was observed in low-density dislocation arrays, in which long-range internal stresses could not be important. There are some indications that cross-slip may be triggered by jogs resulting from the cutting of trees but such a process could not be invoked in all observed cases.

(iii) The last non-planar typical configuration is characteristic of a group of similar dislocations, i.e. with one and the same Burgers vector, developing in a set of parallel slip planes. It appeared that when such a group of more or less concentric dislocation loops grows, the leading dislocations look straight, retaining ⟨110⟩ orientations, while next dislocations exhibit irregular shapes, with cusps and crossings. Hair-pin dipolar configurations and even closed loops could be seen in the wake of moving dislocations. Although x-ray topography was not able to prove it, such irregular shapes were taken as evidence of jogs or superjogs, which might be associated with repeated cross-slip but more probably with point defect absorption/emission at the moving dislocations. Superjogs would act as pinning points and the formation of dipoles would follow. Closed loops are probably the result of further cross-slip closing the dipoles at some point.

Although non-planar slip is a pre-requisite for new source formation, most of the three-dimensional configurations summarized above did not result in dislocation multiplication. In a few cases, dislocation sources were observed. Some are described now.

3.3. Dislocation sources

The first two examples described concern dislocations with the $\frac{1}{2}[1\bar{1}0]$ Burgers vectors ($s = 0.18$). Two examples of sources of primary dislocations will be given after.

3.3.1. Dislocation multiplication near the free surface ($\bar{1}\bar{1}0$) from one half-loop. The sequence of topographs shown in figure 1 was recorded at 1075 K, $\sigma = 22$ MPa, during ~27 min in a sample with B orientation. At $t = 15$ min, one half-loop with $b = \frac{1}{2}[1\bar{1}0]$ can be seen gliding in a $(\bar{1}\bar{1}1)$ plane. Both emerging dislocation segments are 60°; the segment parallel to the surface is screw. A knee can be seen, parallel to [101] at the end of the left segment. The half-loop grows regularly until $t = 23$ min, where a darker contrast appears at the end of the left segment, while the knee disappears. On the third snapshot, taken at $t = 25$ min 15 s, a new half-loop has formed, behind the left segment of the main loop, at the surface at the point where the left segment emerged at $t = 23$ min. This new half-loop has the same $\frac{1}{2}[1\bar{1}0]$ Burgers vector and glides in a $(\bar{1}\bar{1}1)$ plane. On the last two pictures, both half-loops are seen to expand normally, without any pinning point.

Our explanation for this source is as follows (figure 2). Let us assume that the left segment CD was pinned by some unknown obstacle F near the $(\bar{1}\bar{1}0)$ surface. A short screw segment HF developed from the pinning point and cross-slipped in (111) towards the surface (the shear stress, $\tau \sim 4$ MPa, is the same in $(\bar{1}\bar{1}1)$ and (111) and the image force could help). As long as the cross-slipped segment did not reach the surface, the force due to the line tension that it exerts on the point H was opposite to which the segment CH exerts on H. Thus, CH was able to turn around H and to annihilate when meeting the segment FD, leaving possibly a closed loop around F if the obstacle was a particle. As soon as the cross-slipped segment had reached the surface at points H′ and F′, the segment HF now reformed could grow in the $(\bar{1}\bar{1}1)$ initial slip plane, but the points H and F were no longer stabilized by opposite line tensions, so that segments HH′ and FF′ can move together with the new loop, to the left and to the right, respectively.

Because the poles H and F were not stable, such a 'dynamical' source would have produced only one new dislocation.

If this scheme is right, the newly formed half-loop remained connected to the surface by two segments lying in the cross-slip plane. These short segments cannot be resolved by x-ray topography.

3.3.2. Alternative multiplication of $\frac{1}{2}[1\bar{1}0]$ dislocations in (111) and $(\bar{1}\bar{1}1)$. The sequence illustrated in figure 3 was obtained in the same sample as the previous one. At $t = 11$ min, one dislocation, with $b = \frac{1}{2}[1\bar{1}0]$, looks folded, forming a loop, which indicates that it glides partly in (111) and partly in $(\bar{1}\bar{1}1)$. At $t = 19$ min, the two crossing segments have met and formed a closed loop separated from the remaining part of the dislocation which is free to move to the left. No image could be obtained before $t = 23$ min 30 s, at which time the configuration has evolved a lot. A possible scenario is as follows (figure 4).

First, it must be mentioned that the resolved shear-stress on both slip planes was low, $\tau \sim 4$ MPa. At such a stress, 60° segments are approximately twice as fast as screws [6] and dislocations can readily be immobilized from time to time due to local stress fluctuations.

Let us assume that a half-loop gliding in (111) from the $(\bar{1}\bar{1}0)$ surface encounters some obstacle at F (figure 4(a)), which triggers cross-slip of a segment BF in $(\bar{1}\bar{1}1)$ (figure 4(b)). Point B is bound to stay at the intersection of the two glide planes but the line tensions may drive it apart from the fixed point F (figure 4(c)). The segment AF continues gliding in the original (111) plane and the development of cross-slipped segment forms the apparent loop, shown in figure 3(a). When the cross-slipped segment has reached the free surface (figure 4(d)),

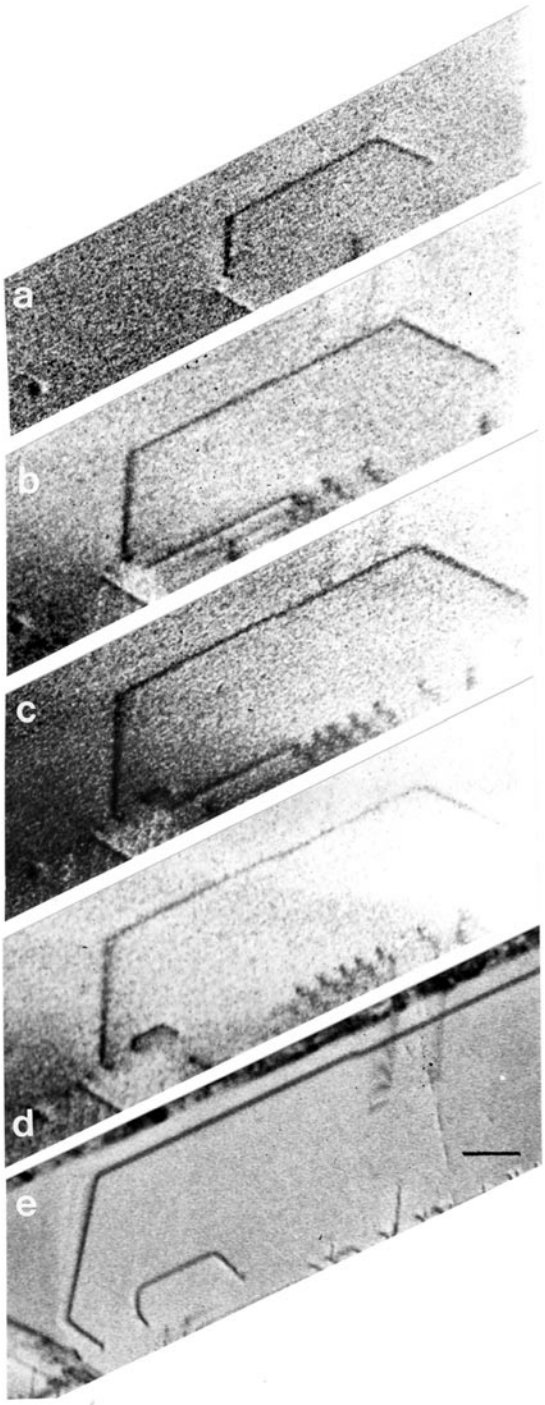

Figure 1. Formation of a new dislocation half-loop near the surface behind an emerging 60° segment of the slip system $[1\bar{1}0](111)$ observed in a sample of B orientation during creep at 1075 K, 22 MPa. Times from the instant of loading: (a) 11 min; (b) 23 min 15 s; (c) 25 min 15 s; (d) 26 min 40 s; (e) 28 min (final state). Marker: 250 μm.

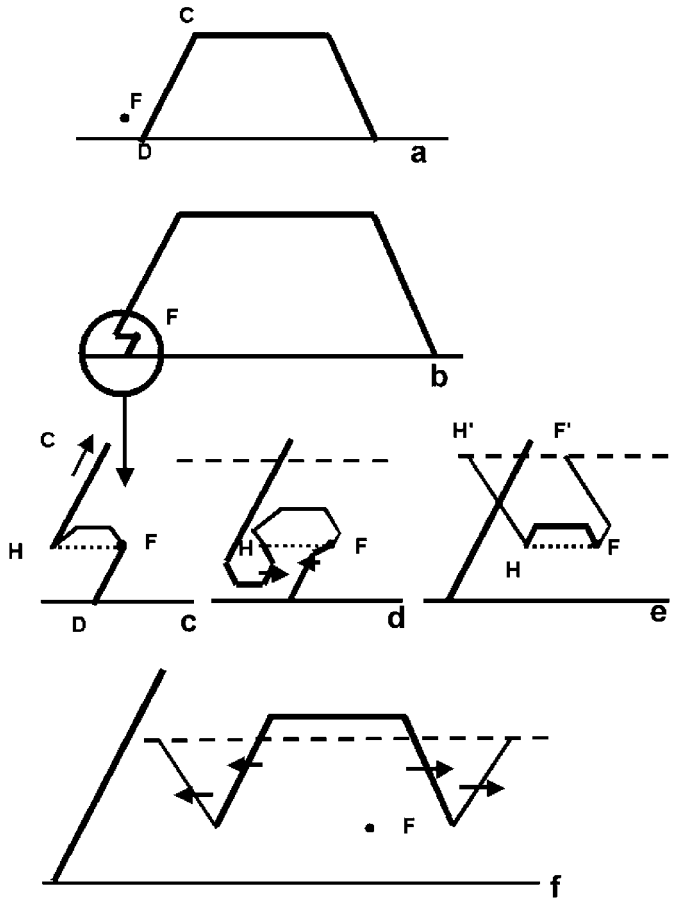

Figure 2. Possible mechanism for the formation of the new half-loop of figure 1. The initial half-loop was in the (111) plane. The segments HF, FF′ and HH′ have cross-slipped in the $(\bar{1}\bar{1}1)$ plane. The broken line in (d)–(f) is the intersection line of the cross-slip plane with the free surface (see text).

the configuration of figure 3(a) is formed. The segments connected to B glide to the right, out of the picture.

In order to explain the separation of the closed loop observed in figure 3(b), one may assume that part of the segment AF did not move, according to the above remark. Meeting of the cross-slipped segment attached to F with that part of the initial segment is then unavoidable (figure 4(e)).

Points H and H′ (figure 4(e)) are not fixed, in contrast to F, and can move freely along the intersection line of planes (111) and $(\bar{1}\bar{1}1)$, depending on the line tensions exerted by the attached segments. It is then possible that gliding segments turn around H and H′ (figure 4(f)) and that new separated loops form when segments of opposite signs meet and annihilate (figure 4(g)). These separated loops always consist of segments gliding in (111) and segments gliding in $(\bar{1}\bar{1}1)$, hence the apparent form of a bean which is visible at $t = 25$ min and 27 min (figure 3) and is reproduced in figure 4(g). Again in this second source configuration, the efficiency of the source is limited by the fact that poles are not fixed but simply stabilized by opposite line tensions exerted by the attached segments.

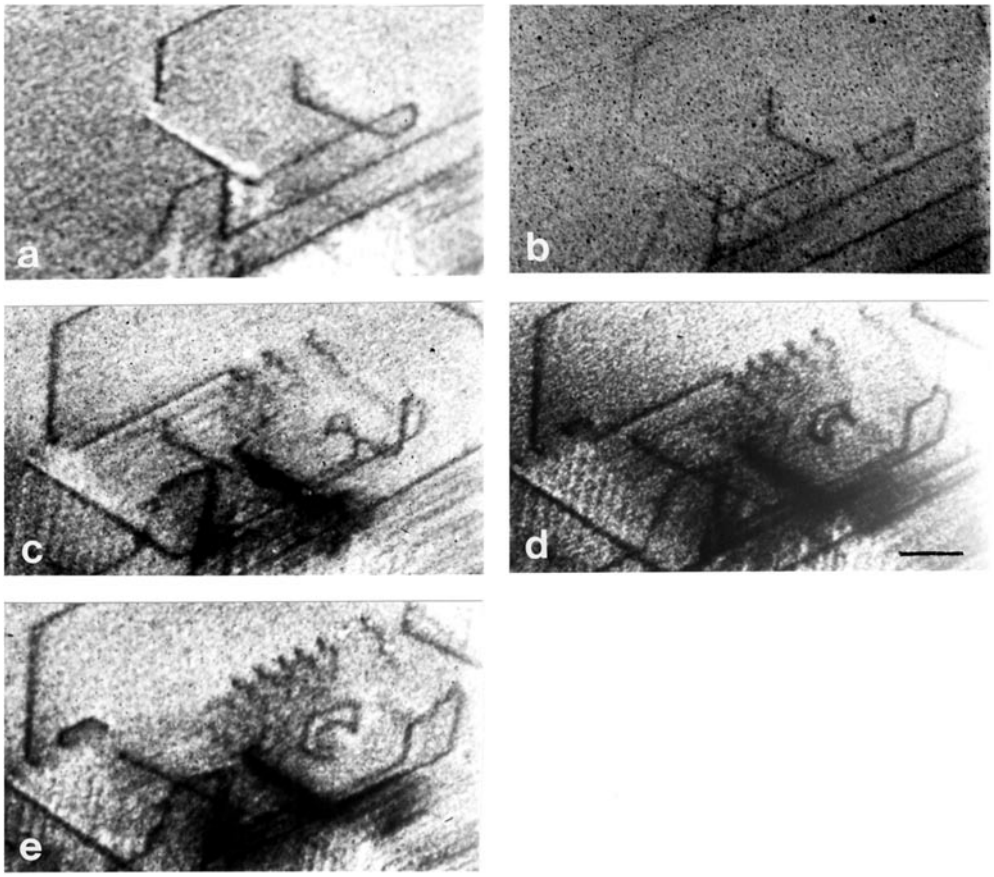

Figure 3. Multiplication of dislocations with $b = \frac{1}{2}[1\bar{1}0]$, alternatively on (111) and $(\bar{1}\bar{1}1)$ planes observed in the same sample as figure 1. Times from the instant of loading: (a) 15 min; (b) 19 min 10 s; (c) 23 min 30 s; (d) 25 min 10 s; (e) 26 min 40 s. Marker: 250 μm.

3.3.3. Sources of primary dislocations. The first example was observed in a sample of orientation A, deformed at 975 K, $\sigma = 22$ MPa for 2 h 40 min. Only the final state is shown in figure 5. Several sets of dislocations have formed at a micro-indent, which gives rise to the black dot contrast. The interesting loop is located in a $(1\bar{1}\bar{1})$ plane. It has a $\frac{1}{2}[101]$ Burgers vector and exhibits zig-zag shapes on the two emerging segments. These zig-zag segments are made of straight $\langle 110 \rangle$ segments, $\sim$50 μm long. At the level of third angular point form the surface, on the left side of the half-loop, a group of smaller concentric half-loops has been formed in a $(1\bar{1}1)$ plane and is marked by an arrow in figure 5(a). These primary loops can be seen well on 111 and 202 topographs.

Such a configuration looks like a classical Frank–Read source (see the attached sketch of figure 5). We assume that at point a, a small segment aa$'$ cross-slipped in the primary plane and has turned around the a and a$'$ poles due to the higher stress in $(11\bar{1})$. Source operation might have been made easier by the vicinity of the $(2\bar{2}\bar{1})$ free surface that emitted loops cut quickly. For such a scheme to work however, a superjog must be present at a$'$, since it is clear that only a limited part of the segment ab cross-slipped in $(11\bar{1})$.

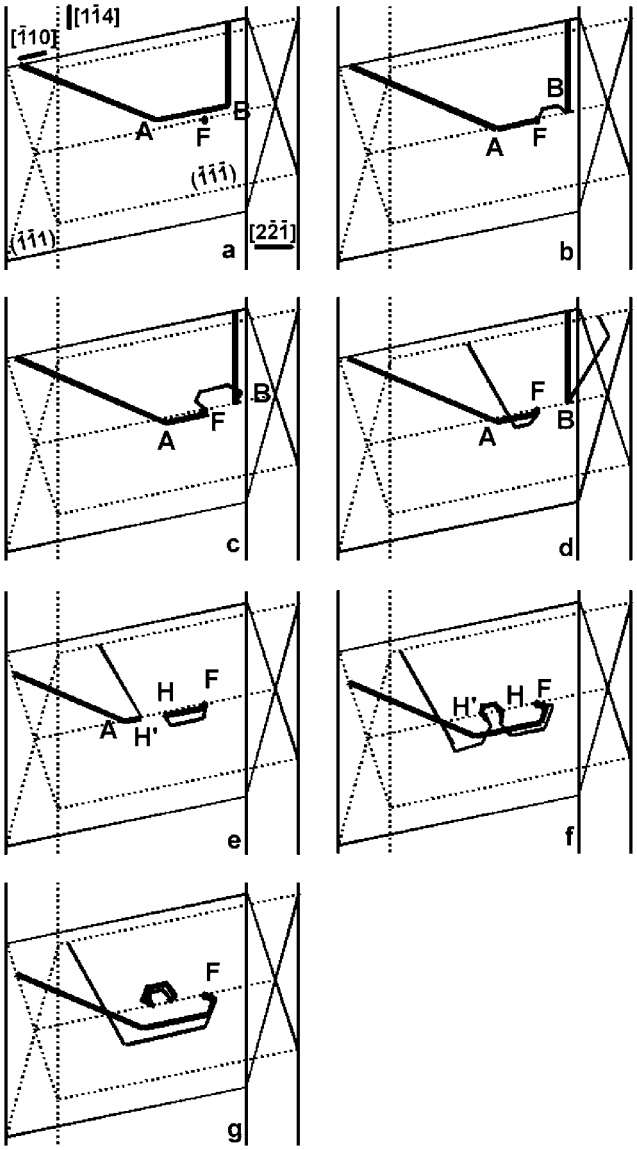

Figure 4. Possible mechanism for the multiplication of dislocations according to the sequence of figure 3. A detailed description is given in the text.

The question here is about the origin and nature of the angular points or cusps on the $\frac{1}{2}[101]$ $(1\bar{1}\bar{1})$ large loop. These cusps are probably the reason for the cross-slip in the primary plane and they provide the necessary anchoring points. It is likely that such cusps are associated with superjogs, which are too short to be measured on the topographs, and it is suggested that constrictions of the dissociated dislocations form at the end of some superjogs.

A second source of primary dislocations is shown in figure 6. It was observed in the same sample of B orientation as the two sources with $b = \frac{1}{2}[1\bar{1}0]$ described above, during a creep at 1075 K, under a tensile stress of 22 MPa.

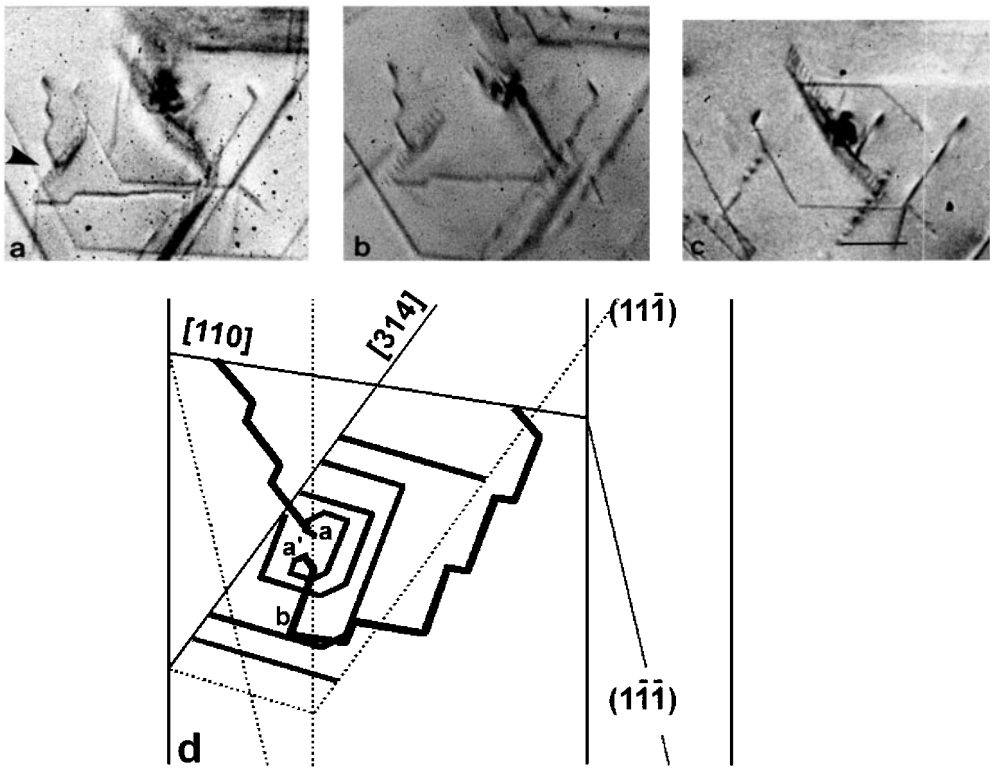

Figure 5. Primary dislocation loops formed on a half-loop of the $\frac{1}{2}[101](11\bar{1})$ slip system. Final state of a sample of A orientation after 2 h 40 min creep at 975 K, 22 MPa. Marker: 250 μm. (a) 202 topograph; (b) 111 topograph; (c) $11\bar{1}$ topograph (the source is out of contrast); (d) sketch (see text).

At the beginning, $t = 1$ min 20 s, two long dislocation lines were already present. They are screw dislocations of the $[1\bar{1}0](111)$ system and had been formed during a previous tensile test, which had to be interrupted for practical problems.

At $t = 11$ min, a group of primary dislocations, belonging to the $[0\bar{1}1](111)$ slip system, has developed from the right side of the sample. The two long segments did not move in the left part of the figure, but did glide in the right part, so that the lower dislocation is now made of two screw segments connected by a short segment parallel to $[\bar{1}01]$. The upper dislocation, which already had a macro-kink, is made of two long screws connected by a curious U-shaped dislocation bulge consisting of three segments: a left one which does not lie along a $\langle 110 \rangle$ orientation, a top one which is screw, and a right one parallel to $[0\bar{1}1]$. This U-shaped configuration will stay apparently immobile during the rest of the test and appears to have been an obstacle in its right side for primary dislocations.

The source appeared on the topograph taken at $t = 17$ min 40 s, just below the acute angle formed at the right side of the U-shaped bulge and above the lower $[1\bar{1}0](111)$ dislocation. It has already emitted, in a (111) plane, at least four concentric loops, which were clearly absent at $t = 11$ min. The source is located at some distance ($\sim$100 μm) below the $(2\bar{2}\bar{1})$ surface. At $t = 23$ min 30 s, the source has emitted about ten loops and the leading ones have already reached the opposite $(\bar{2}21)$ surface. Surprisingly, these emitted loops were blocked at the right side of the U-shaped bulge and could not enter the acute angle it forms with the long $[1\bar{1}0]$

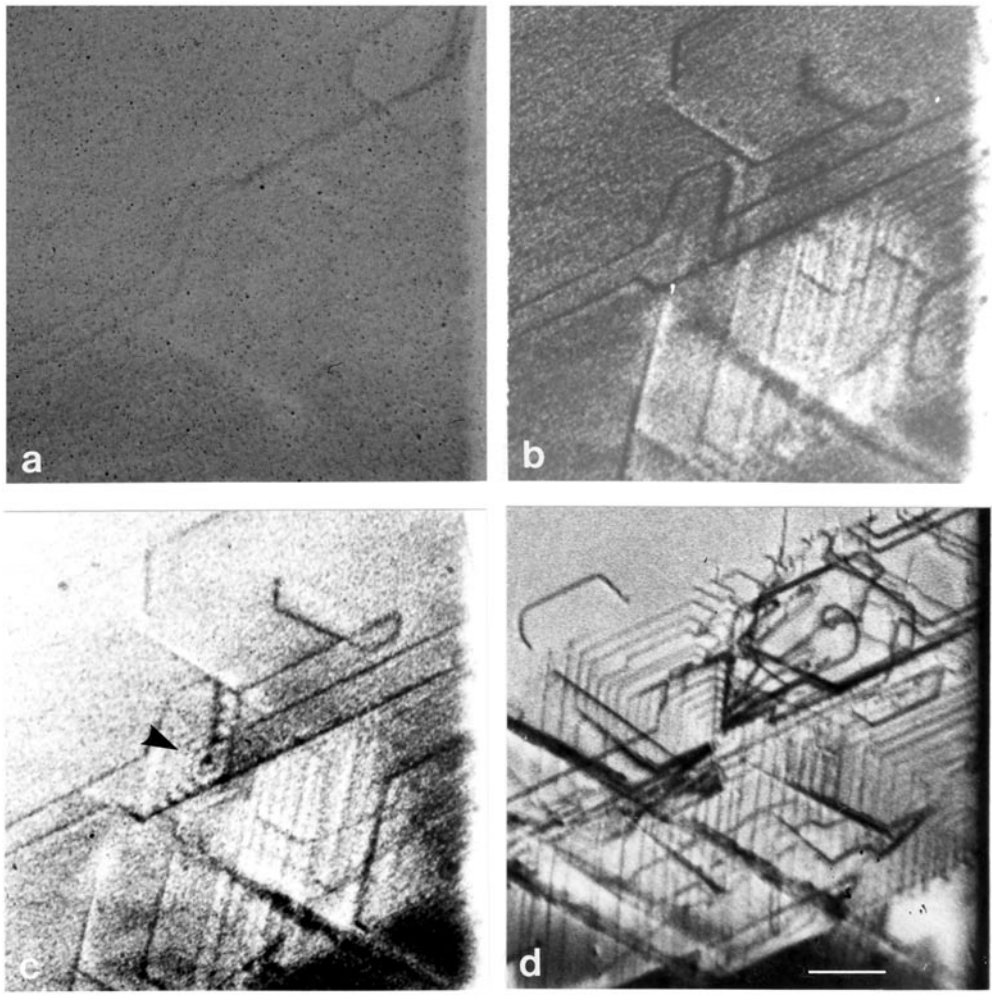

Figure 6. Source of primary dislocations of the $\frac{1}{2}[0\bar{1}1](111)$ slip system observed in the same sample as figure 1. Marker: 250 μm. Times from the instant of loading: (a) 1 min 20 s; (b) 11 min; (c) 17 min 40 s; (d) final state, $2\bar{2}0$ topograph.

screw segment. Accumulation of dislocations along the edges of this angle is made evident from the enhanced dark contrast.

Lang topographs of the final state made sure that the loops emitted by the source have $\frac{1}{2}[0\bar{1}1]$ Burgers vectors.

Remark. During the test, secondary dislocation bands also developed in $(1\bar{1}1)$ planes. They can be seen nearly end-on in the bottom part of topographs. These bands do not seem to play any part in the formation of the source.

A possible scenario for the formation of the source is as follows (figure 7).

Before the source was formed, two sets of dislocations were present in the area and had no interaction with each other: the long screw segments with $b = \frac{1}{2}[1\bar{1}0]$ and the array of primary dislocations $\frac{1}{2}[0\bar{1}1](111)$ created at surface damage on the right (figure 7(a)). For clarity only one long screw, labelled ss, is shown. Primary dislocations essentially consisted of

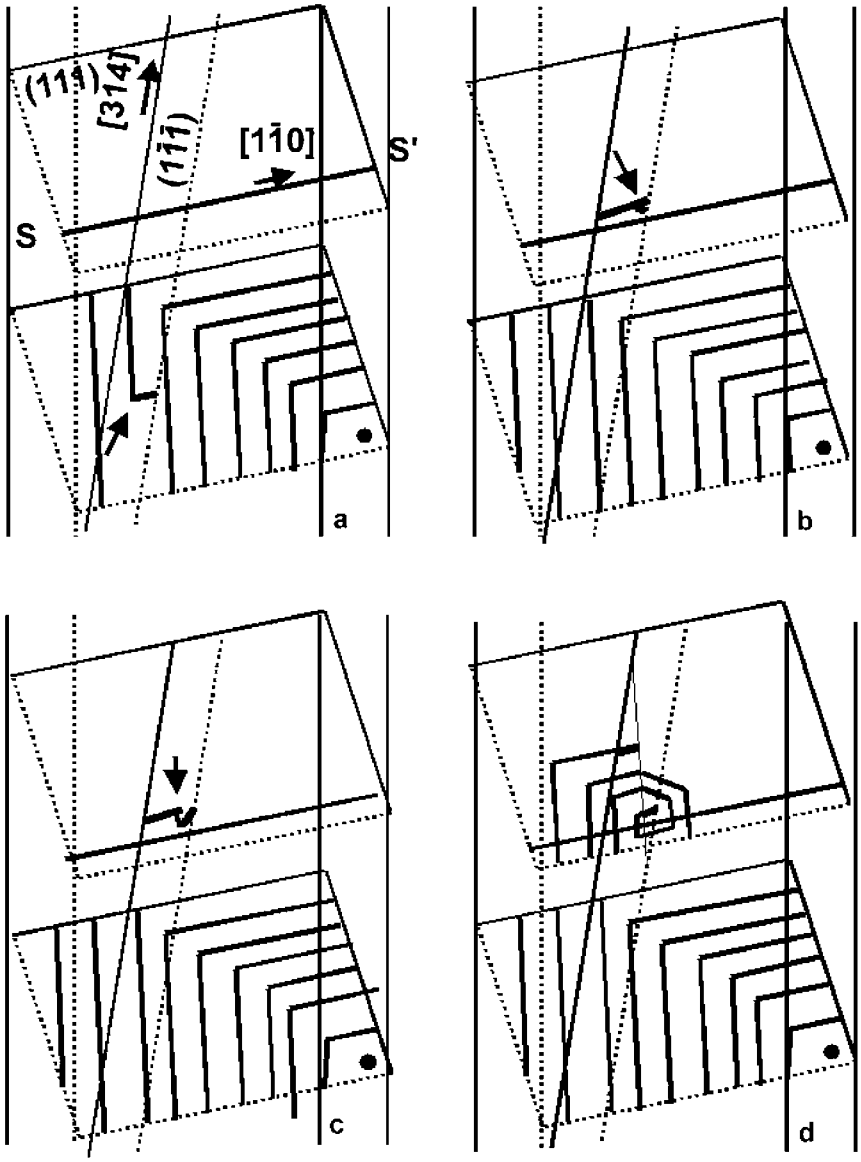

Figure 7. Possible mechanism for the formation of the source of figure 6. Successive events described in the text are marked by arrows.

screw segments connecting the front and rear surfaces of the sample. We make the hypothesis that one of these primary dislocations did cross-slip upwards in ($\bar{1}$11), possibly from the rear surface (figure 7(a)), and was able to escape from the array, being converted into a 60° segment parallel to [110], also connecting the two opposite surfaces.

Such a segment could hardly have been observed in *in situ* topographs, since it would be seen end-on, but the assumed cross-slip event would explain the irregular spacing of dislocations near the head of the array, which was visible from $t = 11$ min.

The cross-slipped segment had soon to cut one of the long screws, which created on it a jog of length $\frac{1}{2}[1\bar{1}0]$ (figure 7(b)). Dragging of this jog led to the formation of a screw segment, parallel to $[0\bar{1}1]$. This last segment is very likely to cross-slip in a (111) plane, on which the shear stress was higher (figure 7(c)). A Frank–Read geometry was then formed provided that poles were sufficiently stable (figure 7(d)). This critical point is better satisfied for sources of primary dislocations, because the stress on the looping arm in that case is at least twice as large as on the anchoring arms.

The piling up of dislocations along some lines, mentioned above, was not explained.

4. Discussion

Observations reported here and in [5] are still far from complete. Because the range of experimental parameters investigated was rather narrow, the temperature and stress dependences of cross-slip and any other mechanisms susceptible to lead to the formation of new sources could not be assessed. Not surprisingly, it appears that non-planar dislocation expansion is more frequent when the temperature is raised, but this observation is purely qualitative. Consequently, a thorough discussion is premature. We just try here to make some remarks and suggestions to complete the work.

Basically, dislocation multiplication in silicon raises two main questions:

(i) What are the sources of the first dislocations?
(ii) How does the crystal fill progressively with dislocations from a few active slip planes? More explicitly, are there fixed preexisting sources which are activated in the stress field of neighbouring dislocations or are there new sources formed by the dislocations themselves? By which mechanisms are these sources formed and in what conditions are they able to operate?

The first question has been voluntarily biased in our experiments, as it was actually biased in most deformation experiments performed so far in semiconductors. In the present work, Vickers indentations and unwanted surface damage, which probably create similar conditions as beneath an indenter, provided the first dislocations. In most other works, dislocations were first created at the ends of the sample which were in contact with compression plates [7].

It is worth noticing that very large volumes of our samples were free of indentations or surface defects and that we have never observed the formation of new loops in such empty regions during a creep test. This is an indication that micro-defects inherited from crystal growth or subsequent thermal treatments do not play a direct role in dislocation production in FZ silicon.

The most probable micro-defects which could be invoked as dislocation sources are A type swirl defects [8], which consist of groups of unfaulted prismatic loops with interstitial character and typical size ranging from 0.5 to 3 μm. Such defects could provide dislocation arms with a size sufficient to form a Frank–Read source in our experimental conditions. The critical stress, τ, to activate a Frank–Read source of diameter d is equal to $\mu b/d$, where μ is the shear modulus and b the modulus of the Burgers vector. A stress of 10 MPa corresponds to a source diameter of $\sim$0.5 μm. Yet, we did not observe such internal sources. A reason might be that our silicon crystals do not contain swirl defects. No indication was obtained on that point from the supplier. A typical density of $\sim 10^6$ cm^{-3} would correspond to $\sim 4 \times 10^4$ defects in one sample.

Regarding the second group of questions, it seems that cross-slip is involved in all configurations described above. Repeated cross-slip was indeed accepted to explain slip band thickening [9] or the propagation of Lüder bands [10]. However cross-slip should

not be as frequently observed if one has in mind that dislocations developed in Si under the present experimental conditions are expected to be widely dissociated, over their whole length. Estimates in the framework of the Escaig model [11] yield prohibitive cross-slip activation energies W, in the bulk and also at a free surface where a narrowing of the core is expected from image force effects [12]. In silicon, under zero stress, W should range between 7.6 and 12.5 eV, depending on some ill defined core parameter in the model. An applied shear stress of 20 MPa should not lower W by more than $\sim$5%. At a pre-existing constriction, W is roughly divided by two.

We believe that cross-slip may start only at existing constrictions and more specifically at dissociated jogs as proposed by Hirsch [13] or at dislocation junctions according to the Washburn mechanism [14]. Some of our observations suggest that a single unit-jog formed by forest cutting might suffice to trigger cross-slip and source formation but all observed cross-slip events cannot be attributed to intersections with trees. The perturbed shapes which appear in dislocation trails could be an indication that jogs may result from point defect absorption or emission by dislocations [5]. Systematic investigation of the core structure of dislocations in silicon crystals deformed in similar conditions could probably be obtained by weak-beam TEM, along the lines of Packeiser's investigation in Ge [15, 16], who was able to measure a density of constrictions and to relate some of them to superjogs.

Once repeated cross-slip has provided a 3D configuration which resembles a Frank–Read source, the efficiency of this potential source, as mentioned above, strongly depends on the stability of the poles. Such unstable or wandering sources were commonly observed in thin foils by *in situ* TEM, e.g. by Louchet in silicon [17]. The stability of these configurations with dislocation segments subjected to variable line tensions is difficult to handle with simple reasoning. It could be treated by numerical simulations like those of Moulin *et al* [4, 18].

Last, we would like to recall previous observations by others of configurations looking similar to those described in this paper, although obtained in less well defined conditions. These observations support our belief that the phenomena reported here are actually playing a role in the beginning of plastic deformation in silicon. The simultaneous development of dislocations in two {111} planes had been observed by Miltat and Bowen [19] and also by Matsui [20] by x-ray topography in wafers deformed by thermal shock. Near surface multiplication of dislocations, without any part of another slip system, as in our figure 1, was observed by Sumino and Harada [21], who performed *in situ* observations by x-ray topography using a high power rotating anode. They also observed a case of multiplication triggered by intersection with a secondary system, which seems to be of the same nature as our figure 6 configuration.

Acknowledgments

Technical help from J P Feiereisen and O Ferry (LPM, Nancy) and from J Baruchel and his group at the ID 19 beam-line at the ESRF is gratefully acknowledged.

References

[1] Dash W C 1956 *J. Appl. Phys.* **27** 1193
[2] Alexander H and Haasen P 1968 *Solid State Phys.* **22** 28
[3] Berner K and Alexander H 1967 *Acta Metall.* **15** 933
[4] Moulin A, Condat M and Kubin L P 1999 *Acta Mater.* **47** 2879
[5] Vallino F, Jacques A and George A *Phys. Status Solidi* a at press
[6] George A and Champier G 1979 *Phys. Status Solidi* a **53** 529
[7] Schröter W, Alexander H and Haasen P 1964 *Phys. Status Solidi* **7** 983

[8] Claeys C and Vanhellemont J 1994 *Advanced Silicon and Semiconducting Silicon Alloys Based Materials and Devices* (Bristol: Institute of Physics) p 35
[9] Mendelson S 1972 *J. Appl. Phys.* **43** 2113
[10] Siethoff H 1973 *Acta Metall.* **21** 1523
[11] Bonneville J and Escaig B 1979 *Acta Metall.* **27** 1477
[12] Möller H J, Ewaldt H and Haasen P 1979 *Phys. Status Solidi* a **55** 469
[13] Hirsch P B 1962 *Phil. Mag.* **7** 67
[14] Washburn J 1965 *Appl. Phys. Lett.* **7** 183
[15] Packeiser G and Haasen P 1977 *Phil. Mag.* A **35** 821
[16] Packeiser G 1980 *Phil. Mag.* A **41** 459
[17] Louchet F 1980 *J. Phys. C: Solid State Phys.* **13** 1847
[18] Moulin A, Condat M and Kubin L P 1997 *Acta Mater.* **45** 2339
[19] Miltat J E A and Bowen D K 1970 *Phys. Status Solidi* a **3** 431
[20] Matsui J 1975 *J. Electrochem. Soc.* **122** 977
[21] Sumino K and Harada H 1981 *Phil. Mag.* A **44** 1319